

# Hydrogen Desorption Properties of Lithium–Carbon–Hydrogen System

Takayuki Ichikawa, Shigehito Isobe\* and Hironobu Fujii

Materials Science Center, N-BARD, Hiroshima University, Higashi-Hiroshima 739-8526, Japan

Hydrogen desorption properties of a mixture of hydrogenated nanostructural graphite  $C^{\text{nano}}H_x$  and lithium hydride LiH are demonstrated in this paper, where  $C^{\text{nano}}H_x$  was synthesized from graphite by ballmilling under 1 MPa hydrogen for 80 h. First of all, we clarified the hydrogenated properties of  $C^{\text{nano}}H_x$  synthesized under four different milling conditions. The hydrogen desorption profile with typical two-peak structure was caused by iron contamination in  $C^{\text{nano}}H_x$  from steel balls during ballmilling, while the products prepared by zirconia balls showed the broad single peak in hydrogen desorption. The amount of desorbed hydrocarbon gas from the products using a rocking (vibrating) mill estimated by the thermogravimetry was larger than that using a rotating (planetary) one. Next, the destabilization properties of extremely stable LiH was examined, indicating that LiH was destabilized by mixing with another component LiOH or NaOH, and then, the mixture easily released hydrogen gas at lower temperature compared with LiH, LiOH and NaOH themselves. On the analogy of this result, we examined hydrogen desorption properties of the ballmilled mixture of LiH and  $C^{\text{nano}}H_x$ . The hydrogen desorption started from about 200°C and showed a peak at 350°C, although each product needs more than 400°C to release hydrogen. Since this hydrogen storage system is specially based on lithium, carbon and hydrogen in the mixture, it can be regarded as Li–C–H hydrogen storage system.

(Received April 22, 2005; Accepted June 8, 2005; Published August 15, 2005)

**Keywords:** hydrogen storage materials, nanostructured graphite, lithium hydride, thermal desorption properties, destabilization

## 1. Introduction

Since Dillon *et al.* reported the hydrogen storage properties of the single walled carbon nanotube,<sup>1)</sup> some carbon-based materials as hydrogen storage media have been extensively investigated all over the world.<sup>2–6)</sup> However, the ability of hydrogen storage due to the physisorption in nanostructural carbons has been recognized not to be suitable for onboard application at room temperature.<sup>7–10)</sup> Actually, temperature below the boiling point of liquid nitrogen is necessary to bring out the hydrogen capacity of more than 5 mass% in carbon-based materials because the trapping energy for the physisorption is estimated to be a few kJ/mol  $H_2$ .<sup>11)</sup> On the other hand, in our previous research, it has been reported that hydrogen storage concentration due to the chemisorption reached up to about 7 mass% in nanostructural graphite  $C^{\text{nano}}H_x$  prepared by mechanically milling for 80 h under 1 MPa hydrogen.<sup>12–16)</sup> However, higher temperature than 700°C is necessary to release all of the chemisorbed hydrogen from  $C^{\text{nano}}H_x$ , because the covalent bond between C and H is too strong to desorb hydrogen.<sup>17)</sup>

In this paper, we report on the issues how to destabilize the Li–H and C–H bonds. First of all, we will clarify the characteristics of  $C^{\text{nano}}H_x$  synthesized by some different methods. Next, the destabilization behavior of extremely stable LiH by mixing with LiOH or NaOH will be discussed, in which the hydrogen desorption takes place at much lower temperature than that of LiH itself. Finally, we will demonstrate how the C–H or Li–H bonding in a mixture of  $C^{\text{nano}}H_x$  and LiH is destabilized by closely contact with each other by ballmilling.

## 2. Experimental

As starting materials, graphite (99.997%) was purchased from Rare Metallic Co. Ltd., whereas LiH (95%), LiOH

(98%) and NaOH (99.998%) were purchased from Sigma-Aldrich. All the samples were treated in an argon glovebox purified by a gas recycling system (MP-P60W, Miwa MFG Co., Ltd.) to minimize the oxygen and water pollution down to a ppm order.

Four kinds of nanostructured graphite were synthesized by planetary (rotating) ballmill (PM, Fritch, P7) or rocking (vibrating) ballmill (SEIWA GIKEN Co. Ltd., RM-10, RM) apparatuses in this work. For each case, 300 mg graphite powder and 20 pieces balls made of steel (7 mm in diameter) or zirconia (8 mm in diameter) were set into a Cr steel vessel, and were milled for 80 h at room temperature under 1 MPa hydrogen. To avoid an increase in temperature during milling process, the ballmilling was interrupted every 1 h and rested for 30 min. At last, these four kinds of samples obtained after the milling treatments were named  $C^{\text{nano}}H_x(\text{Fe}, \text{PM})$ ,  $C^{\text{nano}}H_x(\text{ZrO}_2, \text{PM})$ ,  $C^{\text{nano}}H_x(\text{Fe}, \text{RM})$  and  $C^{\text{nano}}H_x(\text{ZrO}_2, \text{RM})$  as shown in Table 1. Afterwards, LiH was respectively mixed with these four kinds of nanostructured graphite, LiOH and NaOH, after that, these mixtures were ballmilled by the PM apparatus for 2 h under 1 MPa hydrogen.

Gas desorption properties were examined by a thermal desorption mass spectroscopy (TDMS) (Anelva, M-QA200TS) combined with thermogravimetry (TG) and differential thermal analysis (DTA) (Rigaku, TG8120). This apparatus was specially set inside the glovebox, so that the

Table 1 List of sample names, balls kind, milling types and corresponding weight loss values due to 900°C heating in the nanostructural graphite  $C^{\text{nano}}H_x$  prepared under four kinds of ballmilling conditions.

Sample names	Balls	Milling types	TG [mass%] (900°C)
$C^{\text{nano}}H_x(\text{Fe}, \text{PM})$	Steel	Planetary ballmill	13
$C^{\text{nano}}H_x(\text{ZrO}_2, \text{PM})$	ZrO <sub>2</sub>	(Rotation)	6
$C^{\text{nano}}H_x(\text{Fe}, \text{RM})$	Steel	Rocking ballmill	32
$C^{\text{nano}}H_x(\text{ZrO}_2, \text{RM})$	ZrO <sub>2</sub>	(Vibration)	33

\*Graduate Student, Hiroshima University

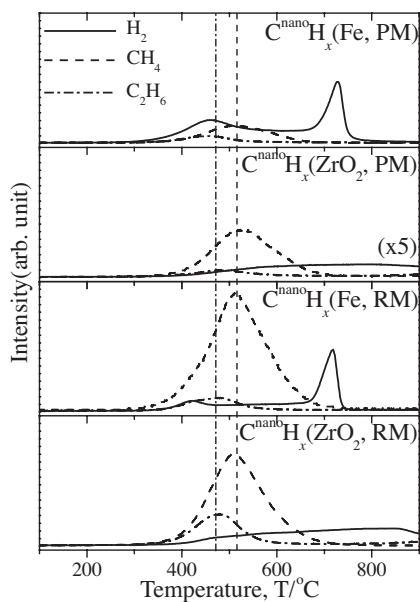


Fig. 1 Hydrogen, methane and ethane desorption profiles of four kinds of nanostructural graphite  $C^{\text{nano}}H_x$ . The examinations were carried out at  $10^\circ\text{C}/\text{min}$  heat rate and under pure helium flow as carrier gas.

measurements of TG, DTA and TDMS could simultaneously be achieved without exposing the samples to air. In this thermal analysis, high-purity helium (purity  $> 99.9999\%$ ) was flowed as a carrier gas, and the heating rate was fixed at  $10^\circ\text{C}/\text{min}$  for four kinds of  $C^{\text{nano}}H_x$  and at  $5^\circ\text{C}/\text{min}$  for six kinds of the mixtures of LiH with four kinds of  $C^{\text{nano}}H_x$ , LiOH and NaOH.

### 3. Results and Discussion

#### 3.1 Thermal gas desorption properties of hydrogenated nanostructural graphite

Figure 1 shows the TDMS profiles of nanostructured graphite prepared under four kinds of milling conditions. The hydrogenated nanostructural graphite milled by steel balls in the planetary mill,  $C^{\text{nano}}H_x(\text{Fe}, \text{PM})$ , or the rocking mill,  $C^{\text{nano}}H_x(\text{Fe}, \text{RM})$ , in which steel scraps were induced as a contamination during milling, showed typical two-peak structure in the hydrogen desorption profiles around  $450$  and  $750^\circ\text{C}$ , while the hydrogenated nanostructural graphite milled by zirconia balls  $C^{\text{nano}}H_x(\text{ZrO}_2, \text{PM})$  and  $C^{\text{nano}}H_x(\text{ZrO}_2, \text{RM})$  had only a broad peak around  $800^\circ\text{C}$ . On the other hand, the desorption profiles of hydrocarbons showed a single peak around  $520^\circ\text{C}$  for the methane gas and  $470^\circ\text{C}$  for the ethane gas independent of the milling methods. It's clear that hydrogen desorption profile of  $C^{\text{nano}}H_x$  is strongly influenced by the iron contamination but the hydrocarbon one is not.

With respect to the TG analyses of the nanostructured graphite up to  $900^\circ\text{C}$ , the products synthesized by the rocking mill revealed much larger values of weight losses than those by the planetary one as shown in Table 1. However, it has been experimentally confirmed that the maximum hydrogen concentration is  $\sim 7\text{ mass}\%$  in milled graphite.<sup>12–16</sup> This indicates that the amount of the hydrocarbon components in the thermally desorbed gases is abundant for nanostructural

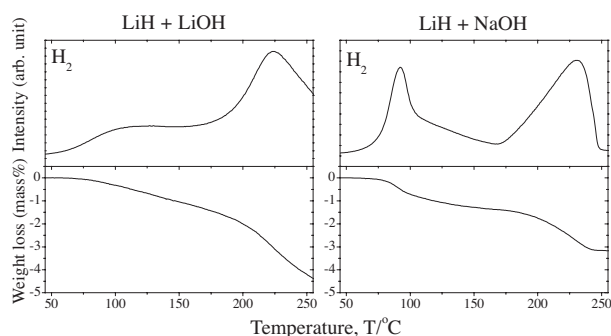


Fig. 2 Hydrogen desorption profile of two kinds of mixtures, LiH + LiOH and LiH + NaOH (upper) and corresponding weight losses (lower). The examinations were carried out at  $5^\circ\text{C}/\text{min}$  heat rate and under pure helium flow as carrier gas.

graphite milled by the rocking mill method because the hydrogen content does not depend on the milling method. From these results, it is concluded that the hydrogenated state in the nanostructural graphite is considerably affected by the milling conditions as well.

#### 3.2 Destabilization properties of extremely stable lithium hydride

It is well-known that lithium hydride LiH is too stable to use for the hydrogen storage media even possessing high hydrogen capacity of  $12.6\text{ mass}\%$ <sup>18</sup> because it has the NaCl type ionic crystal structure. However, this type of ionic structure can be easily destabilized by an interaction with a polar molecule like water or ammonia, leading to hydrogen desorption and to forming, respectively, lithium hydroxide or lithium amide even at room temperature. Therefore, it could be expected that this kind of destabilization takes place on a solid-solid reaction in mixtures of LiH and LiOH or LiH and NaOH.

The TDMS and TG profiles of two kinds of mixtures composed of LiH and LiOH, and LiH and NaOH are shown in Fig. 2. The mixtures desorbed a considerable amount of hydrogen below  $250^\circ\text{C}$ , which indicates the destabilization of all the components, although hydrogen desorption is not expected at these temperatures from each component.

#### 3.3 Hydrogen desorption from mixture of nanostructured graphite and lithium hydride

On the analogy of the above destabilizations due to the interaction between lithium hydride and metal hydroxides, we have regarded the nanostructural graphite  $C^{\text{nano}}H_x$  as a counter product to LiH and have tested whether it is possible to be destabilized by each component. Especially, we have focused on  $C^{\text{nano}}H_x(\text{Fe}, \text{PM})$  and  $C^{\text{nano}}H_x(\text{ZrO}_2, \text{RM})$  as typical products because we would like to obtain an information about an origin of hydrogen desorption from the mixture. As already described above,  $C^{\text{nano}}H_x(\text{Fe}, \text{PM})$  indicated a hydrogen desorption profile with two-peak structure originated in the iron contamination, while  $C^{\text{nano}}H_x(\text{ZrO}_2, \text{RM})$  revealed not typical two peaks but a large amount of weight loss corresponding to the desorption of hydrocarbon. In chemical considerations about the hydrogenated state, the C–H bond in  $C^{\text{nano}}H_x$  has been thought to be the typical covalent bond. However, we have positively

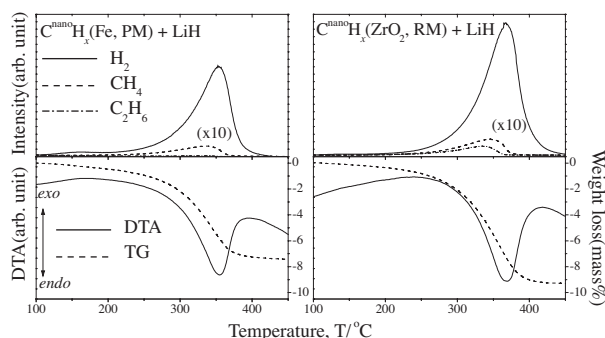


Fig. 3 Hydrogen, methane and ethane desorption profiles of two kinds of mixtures, LiH +  $C^{\text{nano}}\text{H}_x(\text{Fe, PM})$  and LiH +  $C^{\text{nano}}\text{H}_x(\text{ZrO}_2, \text{RM})$  (upper), and corresponding weight losses (TG) and differential thermal analyses (DTA) (lower). The examinations were carried out at  $5^\circ\text{C}/\text{min}$  heat rate and under pure helium flow as carrier gas.

thought it to possessing a polarization in the C–H bond. Actually, we reported that the C–H bond in  $C^{\text{nano}}\text{H}_x$  could be detected as an IR active mode,<sup>19)</sup> indicating that the C–H bond should be polarized.

Figure 3 shows the TDMS, TG and DTA profiles for the ballmilled mixtures of LiH and the above two types of  $C^{\text{nano}}\text{H}_x$ . The hydrogen desorption started at  $\sim 200^\circ\text{C}$  and the peaks of hydrogen and hydrocarbons were located around  $350^\circ\text{C}$ , in which hydrocarbon desorption intensities were  $\sim 10$  times weaker than the hydrogen desorption. Furthermore, it should be noted that the corresponding weight losses from both the mixtures are almost the same, that is, 9 mass% for  $C^{\text{nano}}\text{H}_x(\text{ZrO}_2, \text{RM})$  and 8 mass% for  $C^{\text{nano}}\text{H}_x(\text{Fe, PM})$ , although the weight losses of these  $C^{\text{nano}}\text{H}_x$  products themselves were considerably different as explained above Table 1. It seems likely that the hydrogen desorptions from both the mixtures are of the same origins. Actually, since the peak positions of the hydrocarbon desorption from  $C^{\text{nano}}\text{H}_x$  themselves were not affected by the difference of the above ballmilling conditions, an abrupt disappearance of the hydrocarbon curve above  $350^\circ\text{C}$  suggests that the desorbed hydrogen is mainly originated in the interaction between a liberated hydrocarbon radical and the solid LiH. The DTA result indicates that a clear endothermic peak is synchronized with hydrogen desorption for both the mixtures. Therefore, it is expected to recharge it after dehydrogenation. Actually, we have described that the rechargeable properties of this Li–C–H system is one of the promising candidates for hydrogen storage.<sup>20)</sup>

#### 4. Conclusion

From the examination of the thermal desorption properties in nanostructured graphite  $C^{\text{nano}}\text{H}_x$  prepared under four kinds of ballmilling conditions, it has been clarified that the hydrogenated state in the products is considerably affected by the difference of milling balls and types. The iron contamination caused by the steel balls leads to typical two-peak structure in hydrogen desorption, while the rocking (vibrating) milling brings a large amount of the hydrocarbon gas compared with hydrogen. From the investigation of the hydrogen desorption properties of the LiH and LiOH or LiH

and NaOH mixtures, it has been clarified that it is possible to destabilize the extremely stable LiH by close contact with LiOH or NaOH. On the analogy of these results, we prepared the mixture of  $C^{\text{nano}}\text{H}_x$  and LiH by ballmilling treatment, and then, we examined the thermal desorption properties. The results indicated that both the mixtures desorbed hydrogen below  $350^\circ\text{C}$ , although each product needs more than  $400^\circ\text{C}$  to release all the hydrogen. This hydrogen storage system is specially based on lithium, carbon and hydrogen in the mixture, so that it could be regarded as the Li–C–H hydrogen storage system.

#### Acknowledgement

This work was carried out by the NEDO project “Development for Safe Utilization and Infrastructure of Hydrogen Industrial Technology” in Japan, the Grant-in-Aid for COE Research (No. 13CE2002) of the Ministry of Education, Sciences and Culture of Japan, and the Sasakawa Scientific Research Grant from The Japan Science Society. The authors gratefully acknowledge Mr. K. Nabeta and Mr. S. Hino for their help.

#### REFERENCES

- 1) A. C. Dillon, K. M. Jones, T. A. Bekkedahl, C. H. Kiang, D. S. Bethune and M. J. Heben: *Nature* **386** (1997) 377–379.
- 2) Y. Ye, C. C. Ahn, C. Witham, B. Fultz, J. Liu, A. G. Rinzler, D. Colbert, K. A. Smith and R. E. Smalley: *Appl. Phys. Lett.* **74** (1999) 2307–2309.
- 3) C. Park, P. E. Anderson, A. Chambers, C. D. Tan, R. Hidalgo and N. M. Rodriguez: *J. Phys. Chem. B* **103** (1999) 10572–10581.
- 4) P. Chen, X. Wu, J. Lin and K. L. Tan: *Science* **285** (1999) 91–93.
- 5) C. Liu, Y. Y. Fan, M. Liu, H. T. Cong, H. M. Cheng and M. S. Dresselhaus: *Science* **286** (1999) 1127–1129.
- 6) A. C. Dillon and M. J. Heben: *Appl. Phys. A: Mater. Sci. Process.* **72** (2001) 133–142.
- 7) M. Hirscher, M. Becher, M. Haluska, F. Zeppelin, X. Chen, U. Dettlaff-Weglikowska and S. Roth: *J. Alloys Compd.* **356–357** (2003) 433–437.
- 8) T. Kiyobayashi, H. T. Takeshita, H. Tanaka, N. Takeichi, A. Züttel, L. Schlapbach and N. Kuriyama: *J. Alloys Compd.* **330–332** (2002) 666–669.
- 9) H. Kajiura, S. Tsutsui, K. Kadono, M. Kakuta and M. Ata: *Appl. Phys. Lett.* **82** (2003) 1105–1107.
- 10) H. Takagi, H. Hatori, Y. Soneda, N. Yoshizawa and Y. Yamada: *Mater. Sci. Eng. B* **108** (2004) 143–147.
- 11) A. Züttel, Ch. Nutzenadel, P. Sudan, Ph. Mauron, Ch. Emmenegger, S. Rentsch, L. Schlapbach, A. Weidenkaff and T. Kiyobayashi: *J. Alloys Compd.* **330–332** (2002) 676–682.
- 12) S. Orimo, G. Majer, T. Fukunaga, A. Züttel, L. Schlapbach and H. Fujii: *Appl. Phys. Lett.* **75** (1999) 3093–3095.
- 13) S. Orimo, T. Matsushima, H. Fujii, T. Fukunaga and G. Majer: *J. Appl. Phys.* **90** (2001) 1545–1549.
- 14) D. M. Chen, T. Ichikawa, H. Fujii, N. Ogita, M. Udagawa, Y. Kitano and E. Tanabe: *J. Alloys Compd.* **354** (2003) L5–L9.
- 15) T. Ichikawa, D. M. Chen, S. Isobe, E. Gomibuchi and H. Fujii: *Mater. Sci. Eng. B* **108** (2004) 138–142.
- 16) S. Isobe, T. Ichikawa, J. I. Gottwald, E. Gomibuchi and H. Fujii: *J. Phys. Chem. Solids* **65** (2004) 535–539.
- 17) W. Grochala and P. Edwards: *Chem. Rev.* **104** (2004) 1283–1315.
- 18) F. Schüth, B. Bogdanović and M. Felderhoff: *Chem. Commun.* **20** (2004) 2249–2258.
- 19) N. Ogita, K. Yamamoto, C. Hayashi, T. Matsushima, S. Orimo, T. Ichikawa, H. Fujii and M. Udagawa: *J. Phys. Soc. Jpn.* **73** (2004) 553–555.
- 20) T. Ichikawa, S. Isobe, K. Nabeta and H. Fujii: *Appl. Phys. Lett.* **74** (2005) 241914-1–241914-3.